

Zeitschrift: IABSE reports = Rapports AIPC = IVBH Berichte
Band: 54 (1987)

Artikel: Numerical comparisons involving different 'concrete-models'
Autor: Crisfield, Michael A. / Wills, John
DOI: <https://doi.org/10.5169/seals-41928>

Nutzungsbedingungen

Die ETH-Bibliothek ist die Anbieterin der digitalisierten Zeitschriften auf E-Periodica. Sie besitzt keine Urheberrechte an den Zeitschriften und ist nicht verantwortlich für deren Inhalte. Die Rechte liegen in der Regel bei den Herausgebern beziehungsweise den externen Rechteinhabern. Das Veröffentlichen von Bildern in Print- und Online-Publikationen sowie auf Social Media-Kanälen oder Webseiten ist nur mit vorheriger Genehmigung der Rechteinhaber erlaubt. [Mehr erfahren](#)

Conditions d'utilisation

L'ETH Library est le fournisseur des revues numérisées. Elle ne détient aucun droit d'auteur sur les revues et n'est pas responsable de leur contenu. En règle générale, les droits sont détenus par les éditeurs ou les détenteurs de droits externes. La reproduction d'images dans des publications imprimées ou en ligne ainsi que sur des canaux de médias sociaux ou des sites web n'est autorisée qu'avec l'accord préalable des détenteurs des droits. [En savoir plus](#)

Terms of use

The ETH Library is the provider of the digitised journals. It does not own any copyrights to the journals and is not responsible for their content. The rights usually lie with the publishers or the external rights holders. Publishing images in print and online publications, as well as on social media channels or websites, is only permitted with the prior consent of the rights holders. [Find out more](#)

Download PDF: 12.01.2026

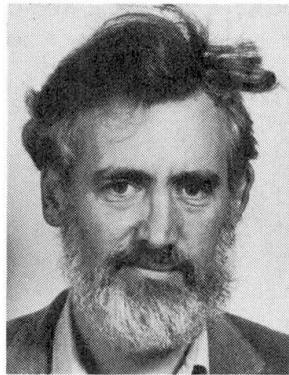
ETH-Bibliothek Zürich, E-Periodica, <https://www.e-periodica.ch>

Numerical Comparisons Involving Different 'Concrete-Models'

Comparaisons numériques sur la base de différents modèles de béton

Numerische Vergleiche verschiedener Beton-Modelle

Michael A. CRISFIELD
Transp. and Road Res.
Lab.
Crowthorne, Berkshire
England



Michael Crisfield obtained both his B.Sc. and Ph.D. at the Queen's University of Belfast. Since that time he has mainly worked at the Transport and Road Research Laboratory on the application of non-linear finite element methods to bridge structures.

John WILLS
Transp. and Road Res.
Lab.
Crowthorne, Berkshire
England



John Wills graduated from Cambridge University in 1955 with a First Class Honours Degree in Mechanical Sciences. He worked for ten years in the gas-turbine research field before joining the Transport and Road Research Laboratory where he is working on the numerical analysis of bridge structures.

SUMMARY

The paper applies different concrete models to the finite element analysis of simple reinforced-concrete panels subject to monotonically increasing states of uniform stress. The panels involve: a) a hypothetical model designed to test the limit-loads when idealised material properties are assumed and b) Vecchio and Collins' experimental panels. The different 'concrete models' involve: 1) fixed orthogonal-cracks, 2) 'swinging cracks' in which the directions of principal stress and principal strain are assumed to coincide, 3) a modification to the previous model whereby the stress in one swinging direction is influenced by the strain in the swinging direction, 4) simple plasticity-models involving both flow and deformation theory which assume no-tension and a 'square yield-criterion'.

RÉSUMÉ

La contribution applique différents modèles de béton pour l'analyse par éléments finis de panneaux simples en béton armé soumis à des contraintes uniformes croissant de façon monotonique. Les panneaux sont définis dans un cas par un modèle théorique analysant les charges limites pour des matériaux idéaux; dans l'autre cas, il s'agit des panneaux expérimentaux de Vecchio et Collins. Les différents modèles de béton prennent en considération les fissures fixes orthogonales; les fissures mouvantes dans lesquelles la direction des contraintes principales et des déformations principales sont les mêmes par hypothèse; une modification du modèle précédent dans lequel la contrainte dans une direction mouvante est influencée par la déformation dans une autre direction; enfin les modèles plastiques simple basés sur la théorie d'écoulement et de déformation, en considérant qu'il n'y a pas de tension et qu'il y a un critère d'écoulement.

ZUSAMMENFASSUNG

Der Beitrag verwendet verschiedene Werkstoffmodelle für Beton bei der Anwendung auf statisch belastete Scheiben. Die Scheiben betreffen einen hypothetischen Fall und die Experimente von Vecchio/Collins. Die Werkstoffmodelle sind: festgelegte orthogonale Risse, Risse in der Richtung der Hauptspannungen bzw. -Dehnungen, Interaktion zwischen Spannung und Dehnung in Rissrichtung und schliesslich ein einfaches Plastizitätsmodell.



1. INTRODUCTION

Most current finite element programs adopt the fixed-orthogonal crack model [1] to treat the cracking of concrete. In this approach, the direction of cracking is governed by the direction of the first principal tensile stress that exceeds the cracking stress. The major drawback of this model involves the development of principal tensile stresses greater than the cracking stress at angles that differ from those of the original two fixed-orthogonal directions. This deficiency arises when the straining is "non-proportional". Even for monotonic, proportional loading, such non-proportional straining is often experienced at the local, Gauss-point level as the adjacent stresses and stiffnesses change. Consequently, the fixed-crack model can give solutions that are far too stiff and collapse loads that are significantly too high [2-4].

Various attempts have been made to allow for non-orthogonal cracks [5-6]. (They are surprisingly few. Non-orthogonal cracks are hardly mentioned in the ASCE review [1]). Of these formulations, the authors considered de Borst's model [5], in which the effect of cracking and plasticity are superimposed, to be most hopeful. However, in attempting to implement this model, the authors encountered significant numerical difficulties when "state changes" occurred within an increment. Difficulties are also associated with discontinuities involving the "threshold angle" [5] beyond which the second non-orthogonal crack is activated.

For these reasons, the authors have, for the time-being, reverted to a simple swinging-crack model [2,4] in which the directions of principal stress and principal strain are assumed to coincide. These models can be criticised [7] for being "un-physical" in that the properties originally relating to a crack, or series of cracks, in one direction are assumed to rotate and relate to a new direction. However, the direction of the principal strain can be considered as relating to the currently-most-active crack for which the properties are influenced by previous adjacent cracks.

Much previous work on reinforced concrete has employed limit-analysis and plasticity with the square yield-criterion [8,9]. The authors have therefore introduced such a yield-criterion into a finite element computer program and have established a close relationship with the simple swinging-crack model. Finally, the basic swinging-crack model has been improved by incorporating the ideas of Vecchio and Collins [10] to degrade the compressive strength as a function of the tensile strain in the orthogonal direction.

2. THE FIXED-CRACK MODEL

Once cracking has occurred, the fixed-crack model is based on the incremental stiffness relationship:

$$\Delta\sigma_{xy} = \begin{bmatrix} \Delta\sigma_x \\ \Delta\sigma_y \\ \Delta\tau_{xy} \end{bmatrix} = \begin{bmatrix} c^2 & s^2 & -2sc \\ s^2 & c^2 & 2sc \\ sc & -sc & c^2 - s^2 \end{bmatrix} \begin{bmatrix} \Delta\sigma_1 \\ \Delta\sigma_2 \\ \Delta\tau_{12} \end{bmatrix} = T(\theta)^T \Delta\sigma_{12} \dots \dots \dots (1)$$

$$\text{or: } \Delta\sigma_{xy} = T(\theta)^T \begin{bmatrix} E_{t1} & 0 & 0 \\ 0 & E_{t2} & 0 \\ 0 & 0 & \beta G \end{bmatrix} \Delta\epsilon_{12} = T(\theta)^T E_{t12} T(\theta) \Delta\epsilon_{xy} \dots (2)$$

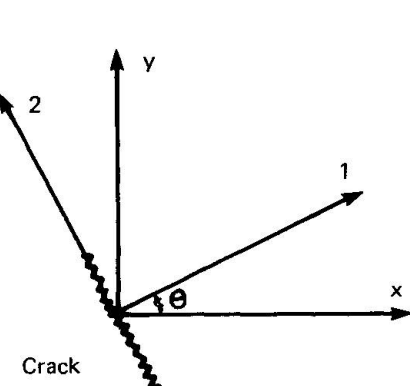


Fig. 1 1-2 and x-y coordinate system

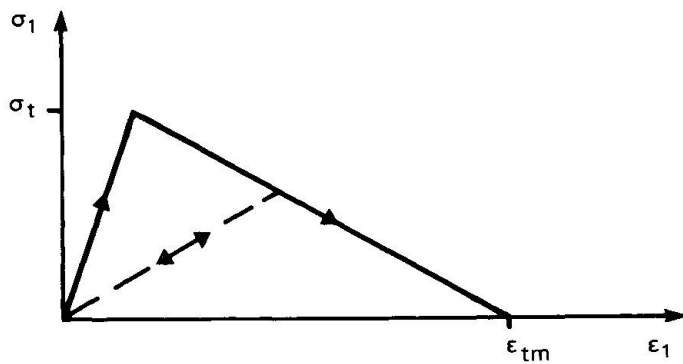


Fig. 2 Concrete softening (tension stiffening)

where $c = \cos\theta$ and $s = \sin(\theta)$ and θ (Fig. 1) is fixed as the direction of the principal stress (σ_1) at first cracking. The terms E_{t1} and E_{t2} in the matrix E_{t12} of (2) are the slopes of the uniaxial stress-strain curves. Immediately after cracking, E_{t1} will be negative to allow for the softening (or tension-stiffening) in tension (Fig. 2). When an incremental step moves from an uncracked to a cracked state, the strain ratio r is computed whereby the old stresses, σ_0 , are augmented by $rE\Delta e$ such that the resulting stresses:

have a principal tensile stress that just reaches the cracking strength. Assuming no plasticity prior to cracking, the matrix E in (4) is the elastic isotropic modular matrix. The remaining strain step $(1-r)\Delta\epsilon$ is applied using equation (2).

3. THE SWINGING-CRACK MODEL

The simplest swinging-crack model assumes that the principal stresses and strains coincide and that:

$$\sigma_{xy} = \begin{bmatrix} \sigma_x \\ \sigma_y \\ \tau_{xy} \end{bmatrix} = T(\theta)^T \begin{bmatrix} \sigma_1(\epsilon_1(\theta)) \\ \sigma_2(\epsilon_2(\theta)) \\ 0 \end{bmatrix} = T'(\theta)^T \begin{bmatrix} \sigma_1 \\ \sigma_2 \end{bmatrix} = T'(\theta)^T \sigma_{12}' \quad .(4)$$

where $T'(\theta)^T$ contains the first two columns of the matrix $T(\theta)$ given in (1) with θ relating to the direction of the continuously varying principal strain. Equation (4) can be differentiated to give:

$$\delta\sigma_{xy} = \left[T'(\theta)^T \begin{bmatrix} \frac{\partial\sigma_1}{\partial\epsilon_1} & \frac{\partial\sigma_1}{\partial\epsilon_2} \\ \frac{\partial\sigma_2}{\partial\epsilon_1} & \frac{\partial\sigma_2}{\partial\epsilon_2} \end{bmatrix} T'(\theta) + \frac{0.5\gamma_{xy}\sin2\theta(\sigma_1 - \sigma_2)}{(\epsilon_x - \epsilon_y)^2 + \gamma_{xy}^2} \begin{bmatrix} 1 & -1 & -\omega \\ -1 & 1 & \omega \\ -\omega & \omega & \omega^2 \end{bmatrix} \right] \delta\epsilon_{xy} \quad .(5)$$

where $\omega = \cot2\theta$. The $\frac{\partial\sigma_1}{\partial\epsilon_2}$ and $\frac{\partial\sigma_2}{\partial\epsilon_1}$ terms in (5) are zero if, as here, (4) is adopted for the total stress-strain relationships. They are included in (5) in order to allow for extensions in the next section. The special form of (5) involving a no-tension material with zero Poisson's ratio and an elastic compressive response was derived by Guptal et al [4]. The tangent modular matrix in (5) follows directly from equation (4) and does not involve the shear-retention factor, β , that is used in (2) for the fixed-crack model.

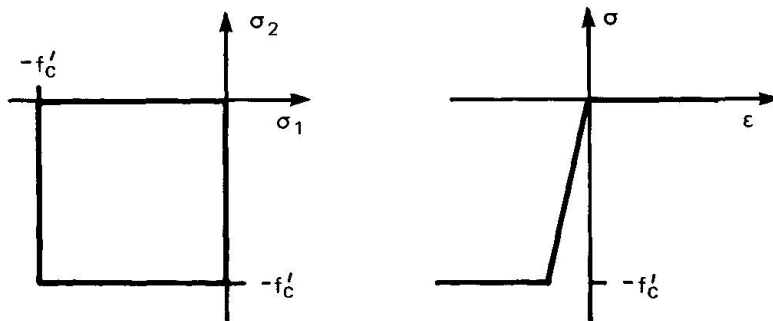
4. A SIMPLE PLASTICITY MODEL

The square yield criterion of Fig. 3(a) has often been used for "limit-load plasticity computations" [8,9] involving reinforced concrete. In its basic form, no tension is allowed and a perfectly plastic response is assumed in compression (Fig. 3(b)) once the compressive strength (say the cylinder strength, f'_c) is reached. Limit-load calculations also consider the elastic strains to be negligible in comparison to the plastic strains but this assumption will not be adopted here. From Fig. 3(a), the yield functions are given by:

$$f = \sigma_1(\theta)\sigma_2(\theta) = (\sigma_1(\theta) - f'_c)(\sigma_2(\theta) - f'_c) = 0 \quad .(6)$$

The principal stresses $\sigma_1(\theta)$ and $\sigma_2(\theta)$ can be related to σ_{xy} using standard transformations and equations (6) become:

$$f = \sigma_x \sigma_y - \tau_{xy}^2 = (\sigma_x - f'_c)(\sigma_y - f'_c) - \tau_{xy}^2 = 0 \quad .(7)$$



(a) Square yield criterion

(b) Idealised stress-strain curve

Fig. 3 Yield criterion and stress-strain relationship for plasticity model

If we consider a deformation theory with Poisson's ratio as zero, application of normality to (7) leads to:

$$\begin{aligned}\sigma_x &= E \left[\epsilon_x - \lambda(\sigma_y - \{f'_c\}) \right] \\ \sigma_y &= E \left[\epsilon_y - \lambda(\sigma_x - \{f'_c\}) \right] \\ \tau_{xy} &= \frac{E}{2}(\gamma_{xy} + 2\lambda\tau_{xy})\end{aligned}\quad \dots \dots \dots \quad (8)$$

where λ is a "plastic-strain multiplier". Depending on the particular part of the yield surface on which the stresses lie, the $\{f'_c\}$ term may or may not be included. Equations (8) can be used to show that:

$$\tan 2\theta = \frac{\gamma_{xy}}{\epsilon_x - \epsilon_y} = \frac{2\tau_{xy}}{\sigma_x - \sigma_y} \quad \dots \dots \dots \quad (9)$$

and hence, as with the previous swinging-crack model, the principal stresses and principal strains coincide. Following this observation, it can be shown that, if both formulations adopt the stress/strain curves of Fig. 3(b), solutions obtained with the swinging-crack equations (4) will coincide with those obtained from the plasticity equations (6)-(8). The authors' computer program adopts an incremental flow-rule so that the σ_x , σ_y , τ_{xy} terms on the left-hand-side of (8) and the ϵ_x , ϵ_y , γ_{xy} terms on the right-hand-side of (8) are replaced by $\Delta\sigma_x$, ... and $\Delta\epsilon_x$, ... respectively. In these circumstances, the directions of the principal stresses and principal strains will only coincide when "proportional straining" has been applied. Consequently, there is no longer a direct relationship with the swinging-crack model. Solutions using deformation rather than flow theory can be obtained numerically by applying the complete load in a single step.

5.0 THE MODIFIED SWINGING-CRACK MODEL

Numerical results have shown that the basic swinging-crack formulation (Section 3.0) leads to overestimates of the strength of panels failing by shear/compression. This finding is consistent with the relationship that has been demonstrated between the basic swinging-crack model and simple plasticity-theory. For, it is well established that an "effectiveness factor" [9] is required to reduce the compressive strengths when applying the latter theory to the limit-analysis of beams failing in shear [9].

The previous swinging-crack model involves no Poisson or biaxial effects. Milford and Schnobrich [3] have introduced these effects into a swinging-crack formulation by adopting the orthotropic stress-strain relationships of Liu et al [11] and a "failure criterion" relating closely to the experimental results of Kupfer et al [12]. For the present we will ignore any enhanced strength in biaxial compression but are concerned to allow for the reduced compressive strength under tension/compression. To this end, we could have followed Milford and Schnobrich and used failure criteria, involving stresses, that are related to the experimental results of Kupfer et al. However, as the concrete softens, the tensile strain will reach ϵ_{tm} in Fig. 2 and the orthogonal tensile stress will be zero. Hence no strength degradation will be introduced. Consequently,



we have followed Vecchio and Collins [10] in adopting a degradation involving the orthogonal tensile strain rather than the orthogonal tensile stress.

The strength degradations have been incorporated into the swinging-crack model by modifying the simple relationship of (4) to:

$$\sigma_{xy} = T'(\theta)^T \begin{bmatrix} \sigma_1(\epsilon_1(\theta), \epsilon_2(\theta)) \\ \sigma_2(\epsilon_1(\theta), \epsilon_2(\theta)) \end{bmatrix} \quad \dots \dots \dots \quad (10)$$

Following from their experimental results on a series of reinforced concrete panels [10], Vecchio and Collins modified the standard compressive parabola to take the form:

$$\sigma_2 = f_c \left[2 \left(\frac{\epsilon_2}{\epsilon_0} \right) - \mu \left(\frac{\epsilon_2}{\epsilon_0} \right)^2 \right] \text{ or } \sigma_2 = \frac{f_c}{\mu} \left[1 - \frac{\left(\epsilon_2 - \epsilon_{2p} \right)^2}{\left(2\epsilon_0 - \epsilon_{2p} \right)^2} \right] \quad \dots (11)$$

depending on whether the compressive strain ϵ_2 is less or greater than the strain $\epsilon_{2p} = \epsilon_0/\mu$ at which the peak stress f'_c/μ occurs. The term ϵ_0 in (11) is the strain corresponding under uniaxial conditions to f'_c . The "reduction factor" $1/\mu$ caused by the orthogonal tensile strains, ϵ_1 , is given by:

These formulae have been incorporated into a modified swinging-crack model and the derivatives $\frac{\partial \sigma_1}{\partial \epsilon_1}$, $\frac{\partial \sigma_2}{\partial \epsilon_2}$ have been used in the tangent stiffness of (5).

However, the terms $\frac{\partial \sigma_1}{\partial \epsilon_2}$, $\frac{\partial \sigma_2}{\partial \epsilon_1}$ have been neglected since they introduce

non-symmetry. In order to make valid comparisons with the fixed and simple swinging-crack models, the first part of eqn. (11) with $\mu = 1$ has been adopted in these models for the stress/strain relationship in compression.

6.0 IDEALISED PANELS

Gupta and Akbar [4] analysed a set of panels of unit dimensions, subject to uniform stress states involving various combinations of N_x, N_y and N_{xy} (Fig. 4(a)). The latter were proportionally increased until failure occurred by yielding of both sets of reinforcement. The computations assumed that the concrete had no tensile strength and behaved elastically in compression while the steel was assumed to act in an elastic/ perfectly-plastic manner.

The non-linear finite element program has been used to analyse one of Gupta and Akbar's panels (Case 4 of [4]). The adopted properties and loadings were:

Percentage of steel, $p_x = 4.232$, $p_y = 0.768$:

$$v = 0, E_c = 20,000 \text{ N/mm}^2, E_s = 200,000 \text{ N/mm}^2, \sigma_{vs} = 500 \text{ N/mm}^2;$$

$$N_x = N_y = 2.5\lambda \text{ N/mm}, \quad N_{xy} = 5.0\lambda \text{ N/mm}.$$

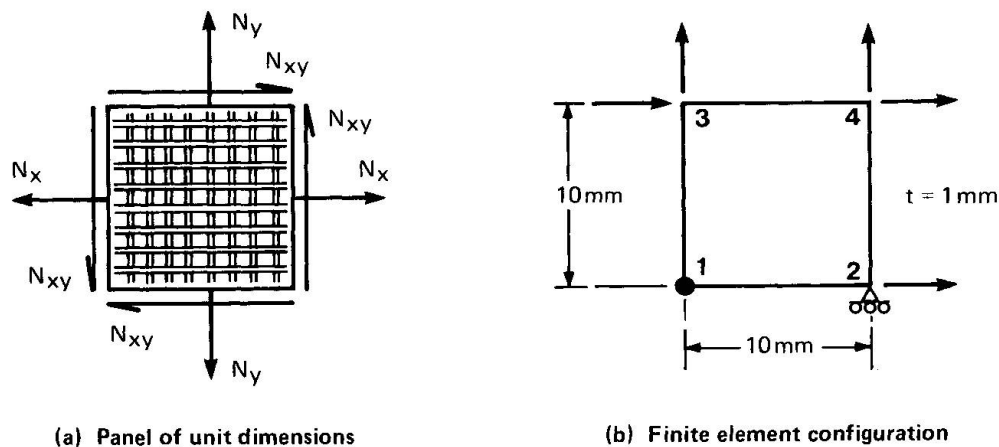


Fig. 4 Idealised panel

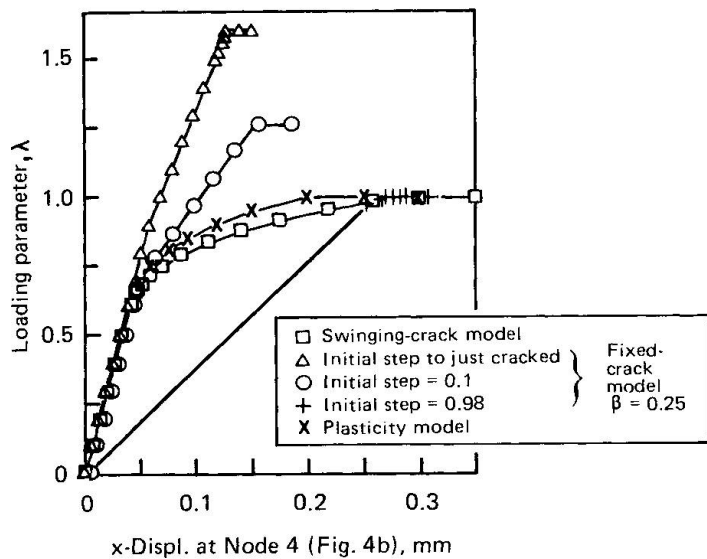


Fig. 5 Load/Deflection relationship for idealised model

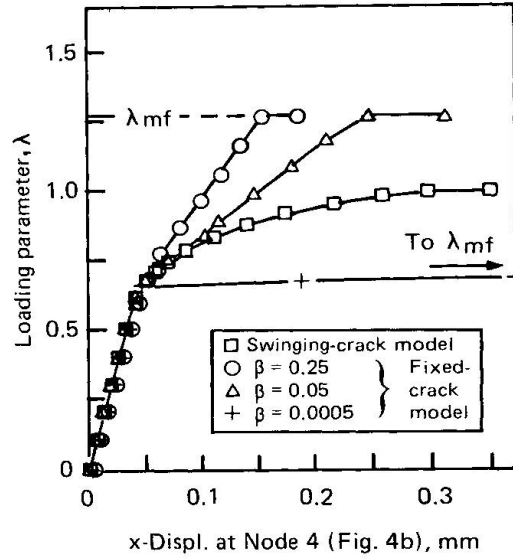


Fig. 6 Influence of shear retention factor, β

where λ is the loading parameter that is unity for the "exact collapse load" [4] obtained from equilibrium and the assumption of no-tension in the concrete. This no-tension condition was approximated by providing a very small tensile strength. In order to produce the simplest possible idealisation and yet use a standard non-linear finite element program, the panel was analysed using a single element with a single Gauss point. The two "mechanisms" were removed via constraint equations.

Fig. 5 plots the loading parameter, λ against the x displacement at node 4 (Fig. 4(b)). It can be seen that both the swinging-crack and plasticity models give the correct collapse load and very similar load/deflection relationships. When the plasticity solutions were obtained in single steps, thus simulating deformation theory, the resulting solutions coincided with the swinging-crack results. For these models, the angle θ (Fig. 1) of the principal tensile stress was 75° when the limit-load was reached. The solutions that were obtained with



the fixed-crack model depended heavily on the initial step-sizes (Fig. 5). For example, when a very small first step was applied, the finite element model provided a crack orthogonal to the principal tensile stress at θ (Fig. 1) = 46.7° . This angle is very close to the angle of the maximum principal stress before cracking. In total contrast, when one single-step was applied almost to the limit-load (using the arc-length method [13]), the fixed-crack model gave a crack orthogonal to $\theta = 75^\circ$ and a solution that lay on the load/deflection curve given by the swinging-crack model. This occurred because, in the limit as the ratio, r , to give first cracking (eqn. (3)) tends to zero, the fixed-crack model (see Section 2) gives:

$$\sigma_{xy} = T(\theta)^T \begin{bmatrix} 0 \\ E\epsilon_2(\theta) \\ \beta G\gamma_{12}(\theta) \end{bmatrix} \quad \dots \dots \dots \quad (13)$$

But θ is given by the principal tensile stress direction of ϵ_{xy} or, equivalently, of ϵ_{xy} . Hence, $\gamma_{12} = 0$ and (13) coincides with (4) which governs the swinging-crack model.

All the fixed-crack solutions obtained in Fig. 5 involved a shear-retention factor, β , of 0.25. Fig. 6. illustrates the effect of varying this factor. It can be seen that, although this parameter affects the load/deflection response, the final collapse load does not depend on β .

7.0 THE PANELS OF VECCHIO AND COLLINS

Numerical analyses have been carried out on five of the thirty panels tested by Vecchio and Collins [10]. These five were chosen with a view to producing a range of failure modes. The adopted compressive stress/strain laws have already been discussed (Section 5). In tension, we normally introduce a simple softening relationship of the form illustrated in Fig. 2. For the current problems, this softening relates to the "tension stiffening" [1,14] which compensates for the inadequacy of the mesh and modelling to capture the shear transfer from the steel to the concrete. Vecchio and Collins have plotted the experimental relationship between the principal tensile stresses and principal tensile strains. From these plots, we have derived a simple relationship of the form of Fig. 2 with $\epsilon_{tm} = 0.004$. This strain is approximately twice the yield strain of the reinforcement.

For the finite element analyses, the panels were idealised using a similar procedure to that described in Section 6 for the "idealised panel". The following models were adopted:

F-CT: the fixed crack model (Section 2) with tensile strength and tension-stiffening and the parabolic compressive stress-strain relationship given by the first part of (11) with $\mu = 1$. The shear-retention factor, β , of (2) is set to 0.25

F-CNT: The fixed-crack model (Section 2) with no tensile strength and a stress/strain relationship as in Fig. 3(b) with an E value of $0.75f_c/\epsilon_0$ and a maximum stress of $0.975f_c$.

S-CT: As F-CT but using the swinging-crack model of Section 3

S-CNT: As F-CNT but using the swinging-crack model of Section 3
 MS-CT As S-CT but using the modified swinging-crack model of Section 5 with compressive stress-strain relationships as in (11)
 MS-CNT As MS-CT but with no tensile strength
 PNT: The plasticity model of Section 4 with no-tension and the idealised compressive stress-strain relationship of model F-CNT

For each analysis, the recorded collapse "loads" are specified (see Table) by means of the maximum shear stress (N/mm^2) applied to the panel. The ratio of $N_x : N_y : N_{xy}$ is given in the Table.

Table: Computed and experimental collapse "loads" (N/mm^2) for the panels of Vecchio and Collins

	PV11	PV19	PV22	PV25	PV27
$N_x : N_y : N_{xy}$	0:0:1	0:0:1	0:0:1	0.69:0.69:1	0:0:1
$\rho_x \sigma_{ysx} / \rho_y \sigma_{ysy}$	1.37	3.83	1.28	1.0	1.0
angles	$45^\circ - 49.5^\circ$	$45^\circ - 63^\circ$	$45^\circ - 48.5^\circ$	$45^\circ - 45^\circ$	$45^\circ - 45^\circ$
Experimental	3.56(Y2)	3.95(S/C+Y1)	6.07(S/C)	9.12(S/C)	6.35(S/C)
F-CT	3.84(Y1) before 3.63(Y2)	5.12(Y2)	7.29(S/C+Y2)	9.72(S/C)	7.89(Y2)
F-CNT	3.61(Y2)	4.67(Y2)	7.27(Y2)	9.28(S/C)	7.89(Y2)
S-CT	3.78(Y1) before 3.59(Y2)	4.18(Y2)	7.24(Y2)	9.72(S/C)	7.89(Y2)
S-CNT	3.59(Y2)	4.18(Y2)	7.24(Y2)	9.28(S/C)	7.89(Y2)
MS-CT	3.69(Y1) before 3.59(Y2)	3.40(S/C+Y1)	5.71(S/C)	7.65(S/C)	5.96(S/C)
MS-CNT	3.59(Y2)	3.39(S/C+Y1)	5.69(S/C)	7.15(S/C)	5.95(S/C)
PNT	3.59(Y2)	4.18(Y2)	7.24(Y2)	9.28(S/C)	7.89(Y2)

S/C = shear/compression failure in concrete

S/C + Y1 = shear/compression failure in concrete + yielding of one set of steel

Y1 = failure by yielding of one set of steel

Y2 = failure by yielding of both sets of steel

In producing these results, an arc-length solution procedure [13] was adopted and hence the limit-loads could be well established without any failure in the iterative solution technique. Also, local limit-loads could be overcome. This is apparent from the numerical results given in the Table for panel PV11 which was the only one to fail exclusively by steel yielding. These local



limit-points could have been removed by reducing the tension-stiffening.

Of all the methods tested, only the modified S-C models (MS-CT and MS-CNT) consistently gave the same collapse modes as those observed in the experiments. These models also gave good or conservative predictions for the collapse strength. The more basic swinging-crack models (S-CT and S-CNT) overestimated the collapse load by about twenty per cent for two of the panels (PV22 and PV27). The fixed-crack models were equally bad in these instances and additionally gave an overestimate of thirty per cent for panel PV19 in which, because the ratio $\rho_x \sigma_{ysx} / \rho_y \sigma_{ysy}$ was high, there was a significant change in the angle of the principal strains.

For every panel, the simple plasticity-model, PNT, gave collapse loads that, as anticipated, coincided with those given by the simple S-C model with no-tension (S-CNT) although, for PV19, in which a significant "swing" occurred, there was some difference in the computed load/deflection" response. However, as predicted, these differences were eliminated when single large-steps were used for the model PNT.

Milford and Schnobrich [3] rejected the use of Vecchio and Collin's strain-related compressive strength degradations because "predicting compression related failures is very sensitive to the tension-stiffening". However, the present results indicate that even the use of a no-tension model in conjunction with the "degraded compression curves" gives reasonable, safe solutions.

8. CONCLUSIONS

The following tentative conclusions have been derived from the numerical tests that have been described. More tests will be required to substantiate these findings.

1. When the straining is non-proportional, the fixed-crack model may give excessively high collapse loads because the crack directions are totally governed by the early straining. However, in some circumstances, the introduction of large step-sizes will reduce the stiffness so that the solutions tend towards those of the swinging-crack model.
2. For steel-dominated ductile failures, the computed load/deflection response, but not the final collapse load, will depend on the shear-retention factor, β , if the fixed-crack model is adopted.
3. If deformation-theory is combined with plastic approach involving the square yield-criterion, the results will coincide with those obtained from an equivalent swinging-crack model. If flow-theory is adopted, the results will often be very similar.
4. A tangent stiffness matrix that is consistent with the swinging-crack model does not require the provision of a shear-retention factor, β .
5. The simple swinging-crack model may overestimate the strength and incorrectly assesses the failure modes of panels failing due to shear/compression.
6. This deficiency can be overcome by providing a compressive stress-strain relationship, similar to that proposed by Vecchio and Collins [10], whereby the compressive strength is reduced by the presence of orthogonal tensile strains (not stresses). Unfortunately this leads to a non-symmetric tangent stiffness matrix that must be symmetrically approximated if efficient solutions are to be obtained. It is probable that an equivalent plasticity-model would involve a non-associative flow-rule.
6. Depending on the choice of tension-stiffening, local limit-points may well be encountered and it is essential to use a numerical solution procedure that will handle these phenomena.

7. In the absence of a simple, but effective fixed-crack model that allows for multiple and non-orthogonal cracks, the modified swinging-crack model appears to offer many advantages. Much further theoretical and experimental work is required on the development of effective stress/strain relationships in both tension and compression. These will need to be functions of both the mesh size and the vicinity and nature of the reinforcement.

9. ACKNOWLEDGEMENTS

The work described in this paper forms part of the programme of the Transport and Road Research Laboratory and is published by permission of the Director.

Crown copyright. Any views expressed in this paper/article are not necessarily those of the Department of Transport. Extracts from the text may be reproduced except for commercial purposes, provided the source is acknowledged.

10. REFERENCES

1. ASCE, Finite element analysis of reinforced concrete: state-of-the-art report, Struct. Div., Committee on Conc. & Masonry Structs., ASCE, New York, 1982.
2. COPE, R.J., RAO, P.V., CLARK, L.A. & NORRIS, P., Modelling of reinforced concrete behaviour for finite element analysis of bridge slabs, in: Numerical Methods for Nonlinear Problems, ed. C. Taylor et al., Pineridge Press, Swansea, Vol. 1, 1980, pp.457-470.
3. MILFORD, R.V., & SCHNOBRICH, Nonlinear behaviour of reinforced concrete cooling towers, Report ISSN: 0069-4274, University of Illinois, May 1984.
4. GUPTA, A.K. & AKBAR, A., Cracking in reinforced concrete analysis, J.of Struct. Div., ASCE, 110, 1984, pp.1735-1746
5. DE BORST, R. & NAUTA, P., Non-orthogonal cracks in a smeared finite element model, Engineering Computations, 2, 1985, pp.35-46
6. ONATE, E., OLIVER, J., & BUGEDA, G., Finite element analysis of the response of concrete dams subjected to internal loads, Finite Element Methods for Nonlinear Problems, ed. P.G. Bergan et al., Springer-Verlag, Berlin, 1985, pp. 653-672.
7. BAZANT, Z.P., Comment on orthotropic models for concrete and geomaterials, J. of Eng. Mech. Div., ASCE, 109, 1983, pp.849-865.
8. NEILSON, M.P., Yield conditions for reinforced concrete shells in the membrane state, Non-classical Shell Problems, Proc. IASS Symp., North-Holland, Amsterdam, 1963, pp.1030-1040.
9. MARTI, P., Plastic analysis of reinforced concrete shear walls, Introductory Report of IABSE Colloq. on Plasticity in Concrete, Zurich, 1979, pp.51-69.
10. VEOCHIO, F. & COLLINS, M.P., The response of reinforced concrete to in-plane shear and normal stresses, ISBN 0-7727-7029-8, Pub. No. 82-03, University of Toronto, 1982.
11. LIU, T.C.Y., NILSON, A.H. & SLATE, F.O., Biaxial stress-strain relations for concrete, J. Struct. Div., ASCE, 98, 1972, pp.1025-1034.
12. KUPFER, H. & GERSTLE, K.N., Behaviour of concrete under biaxial stresses, J. Engng. Mech. Div., ASCE, 99, 1973, pp.852-866.
13. CRISFIELD, M.A., A fast incremental/iterative solution procedure that handles snap-through, Comp. & Structs., 13, 1981, pp.55-62.
14. SCANLON, A. & MURRAY, D.W., Time dependant reinforced concrete slab deflectins, J. Struct. Div., ASCE, 100, 1974, pp.1911-1924

Leere Seite
Blank page
Page vide